

## REDUCTION OF NITRATE BY Fe<sup>2+</sup> IN CLAY MINERALS

VIBEKE ERNSTSEN

Geological Survey of Denmark and Greenland, Thoravej 8, DK-2400, Copenhagen NV, Denmark

**Abstract**—In the 12 km<sup>2</sup> catchment area of Syv creek, Denmark, moderate to high concentrations of nitrate (NO<sub>3</sub><sup>-</sup>) occurred in the upper part of the oxidized zone (oxic-I), but dropped within the lower suboxic part (oxic-II), to below the detection limit in the unoxidized zone. Structural Fe<sup>2+</sup> in the clay minerals made up 10 to 12% of the Fe in the oxidized zone and increased to approximately 50% in the unoxidized zone. Concurrent with changes in the distribution of structural Fe<sup>2+</sup> the clay mineral constituents changed. Vermiculite was typically found in the oxidized zone whereas chlorite was found in the unoxidized zone only. A conversion of illite and chlorite into vermiculite seems to take place. A significant correlation between NO<sub>3</sub><sup>-</sup> and the amount of reduced Fe<sup>2+</sup> in the suboxic (oxic-II) zone, indicates that primary structural Fe<sup>2+</sup> in the clay minerals is the reductant in a NO<sub>3</sub><sup>-</sup> reduction process.

**Key Words**—Chlorite, Clayey till, Exchangeable ferrous iron, Illite, Mössbauer, Nitrate, Oxidized, Structural ferrous iron, Unoxidized, Vermiculite, Weichselian, X-ray.

### INTRODUCTION

In Denmark more than 95% of the public water supplies come from ground water sources, and until now only treatment on a limited scale has been necessary before the ground water is distributed to the consumers. More than 65% of the country is under intensive agricultural production. The addition of increasing amounts of nitrogen fertilizers has resulted in a growing risk of NO<sub>3</sub><sup>-</sup> contamination of the ground water.

Normally the concentration of NO<sub>3</sub><sup>-</sup> in drainage water below the root zone does exceed the European Union (EU) maximum admissible concentration for drinking water. Nevertheless, low concentrations of NO<sub>3</sub><sup>-</sup> are found in ground water in confined aquifers covered by thick layers of clayey sediments (Christensen 1970; Jacobsen 1995) and therefore, NO<sub>3</sub><sup>-</sup> reduction seems to take place.

Few studies in Denmark have focused on NO<sub>3</sub><sup>-</sup> reduction in clayey sediments. Christensen (1970) stated that NO<sub>3</sub><sup>-</sup> is reduced by soluble Fe<sup>2+</sup> in the reduced ground water. For 2 profiles to depths of 20 m below arable land, Lind and Pedersen (1976) showed that NO<sub>3</sub><sup>-</sup> occurs in considerable amounts in the upper oxidized zone, whereas the NO<sub>3</sub><sup>-</sup> content was low within the underlying unoxidized zone. Exchangeable Fe<sup>2+</sup> within the unoxidized clayey till was described as essential for the NO<sub>3</sub><sup>-</sup> reduction when considered as a chemical process. Similarly, studies on 3 profiles in clayey till to depths of 21 meters below agricultural land showed that NO<sub>3</sub><sup>-</sup> occurred in the oxidized zone only. Primary structural Fe<sup>2+</sup> in the clay minerals was postulated to be of importance for NO<sub>3</sub><sup>-</sup> reduction in organic-poor clayey till (Ernstsen and Lindgreen 1985; Ernstsen 1989; Ernstsen and Mørup 1992) with low biological denitrification activities (Zeuthen et al. 1991).

Also for clayey till of southern Alberta, Canada, Hendry et al. (1984) demonstrated a close correlation

between the redox environment and the distribution of NO<sub>3</sub><sup>-</sup>, that is, high concentrations of NO<sub>3</sub><sup>-</sup> in oxidized till and low concentrations within unoxidized clay. The biological denitrification rates were low for samples from both oxidized and unoxidized till and increased rates were primarily localized within fractures with facilitated transport of organic matter from the soil surface or adjacent inherent fragments of organic matter (micro-sites) (Fujikawa and Hendry 1991).

To improve our knowledge of the impact of surface-applied N on the ground water quality for areas dominated by clayey till, the distribution of NO<sub>3</sub><sup>-</sup> and mechanisms of NO<sub>3</sub><sup>-</sup> reduction were studied for the catchment area of Syv creek.

### MATERIALS AND METHODS

#### Site Description

The study area, the catchment area of Syv creek, is located 45 km southwest of Copenhagen, Denmark (Figure 1). The area is under intensive agricultural production.

Ten to 60 of clayey till deposited during the Young Baltic advance of the Middle Weichselian Glaciation (14 to 15 Ka B.P.) cover the confined aquifers (Houmark-Nielsen 1987; Ernstsen et al. 1990). The clay content of the clayey till varies between 10% and 20% (calculated on material <2 mm) and the amount of organic matter in this type of sediment is low, typically 0.2 to 0.4% C (Lind and Pedersen 1976; Ernstsen 1989). Free CaCO<sub>3</sub> occurs below the root zone and pH(CaCl<sub>2</sub>) was 7.7 to 7.8 (Ernstsen et al. 1990).

#### Sample Collection

Eleven profiles (SBI-SBXI) were examined within the 12 km<sup>2</sup> catchment area of Syv creek (Figure 1) and sediment samples were collected to depths of 29 m. The samples were stored frozen until chemical and mineralogical analysis.

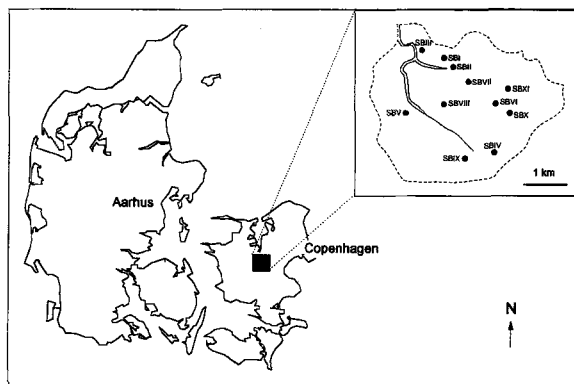


Figure 1. The catchment area of Syv creek, Denmark, with study sites SBI-SBXI.

Methods

The color of the sediment samples were described after the Munsell Soil Color Chart (Munsell Color Company 1976). Nitrate and exchangeable NH<sub>4</sub><sup>+</sup> were extracted from sediment samples with 2M KCl (2 ml extractant/g sediment). Structural Fe<sup>2+</sup> and Fe<sup>3+</sup> within clay minerals and free Fe oxides were investigated by <sup>57</sup>Fe Mössbauer spectroscopy at 77K, exchangeable Fe<sup>2+</sup> was extracted from samples (2 ml extractant/g sediment) with a 3% AlCl<sub>3</sub> solution (Lind and Pedersen 1976) and the amount of Fe in the subsoil was determined by Atomic Adsorption Spectroscopy (AAS) after digestion with HF. Semi quantitative clay

mineralogy was determined by X-ray diffraction (XRD) analysis of clay fractions. The sediment samples were pretreated with sodium acetate at pH 5.0 to remove carbonate. The clay fraction was separated into fine clay (<0.2 μm) and coarse clay (0.2 to 2 μm) using a continuous-flow centrifuge. Iron and Al oxides were removed by Na-citrate/Na-bicarbonate/Na-dithionite (Mehra and Jackson 1960). Diffractometer mounts were prepared by the pipette method with 20 mg sample per cm<sup>2</sup>. The specimens analyzed were Mg<sup>2+</sup>- or K<sup>+</sup>-saturated air-dried specimens, Mg<sup>2+</sup>-saturated and glycerated specimens and K<sup>+</sup>-saturated specimens heated for one hour at 300 °C. Identification of the different groups of minerals was as follows: oxidized zone 7.1 Å, kaolinite; unoxidized zone 7.1 Å, kaolinite and chlorite; 9.8 Å, illite; 13.8 Å-glycerol (oxidized zone), vermiculite; 13.8 Å-glycerol (unoxidized zone), vermiculite and chlorite; 13.8 Å-300 °C (unoxidized zone), chlorite; and 18.2 Å, smectite. Mixed-layered illite-smectite was identified by increased peak intensity between 9.8 Å and 14.0 Å for air-dried Mg-treated samples. The clay mineral compositions were calculated by relative reflection intensities. The total clay reflection area was normalized to 100%. The age of pore-water was determined by its tritium (<sup>3</sup>H) content.

RESULTS

Color and Redox Environment

The profiles were subdivided by color (matrix and mottles) into oxidized and unoxidized redox environ-

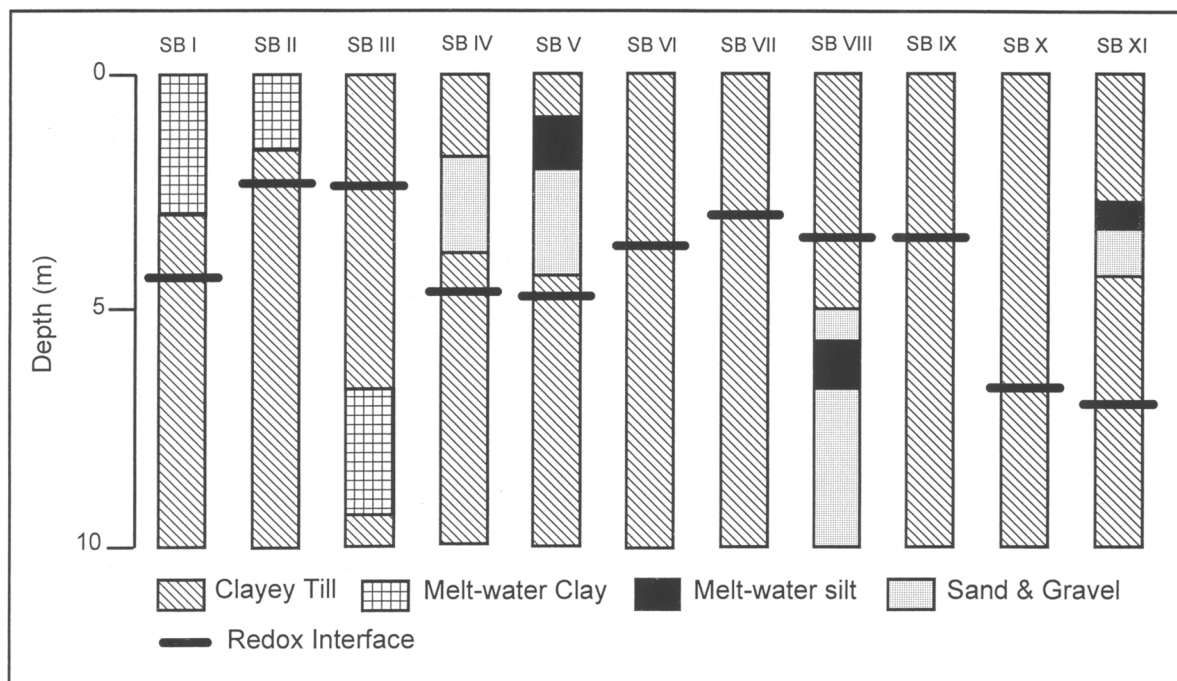


Figure 2. Geology and redox interface (the transition between the oxidized and unoxidized zone) in profile SBI-SBXI.

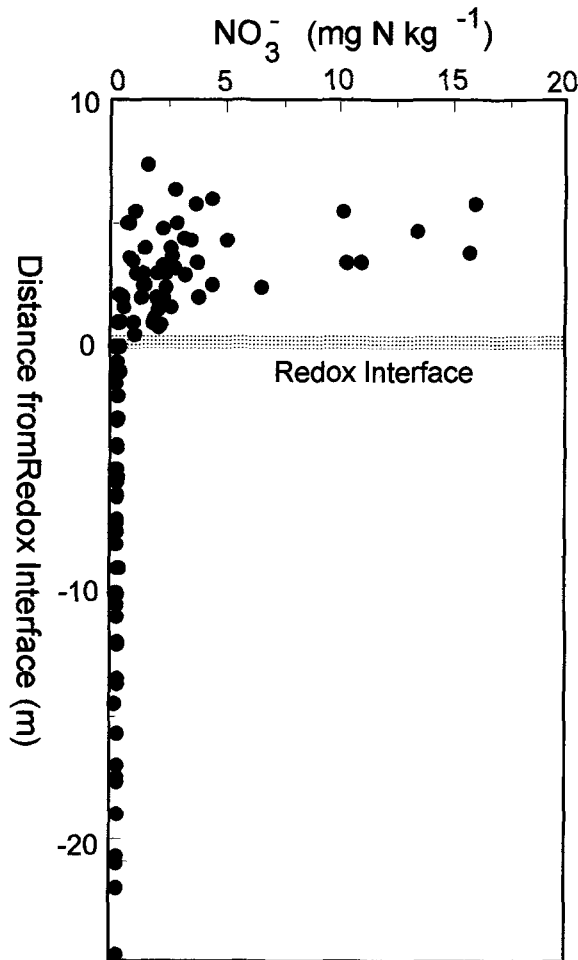


Figure 3.  $\text{NO}_3^-$  vs. depth relative to redox interface. Data from profiles SBI-SBXI.

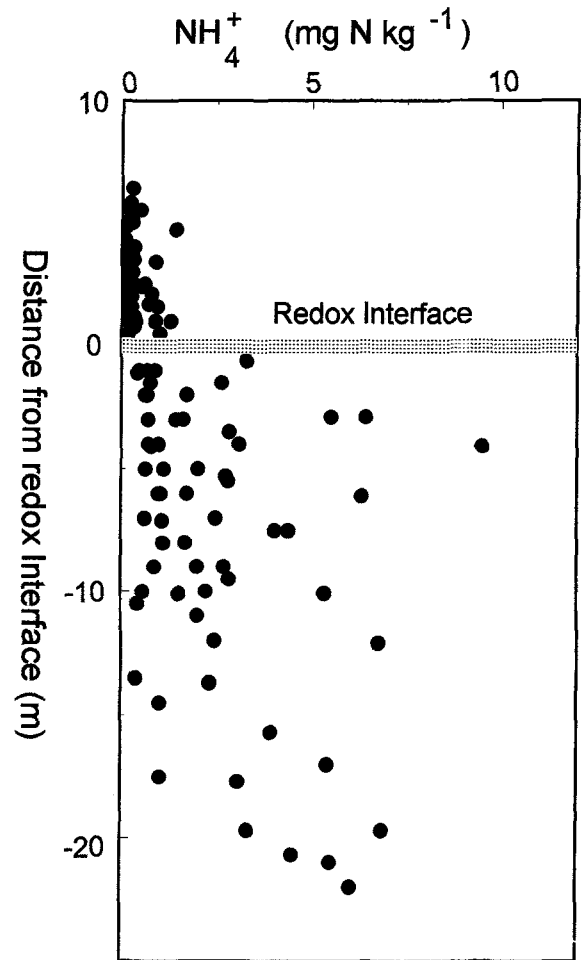


Figure 4. Exchangeable  $\text{NH}_4^+$  vs. depth relative to redox interface. Data from profiles SBI-SBXI.

ments (Figure 2). The oxidized zone was at SBII and SBIII about 2.5 m deep, grey (5Y 7/2 or 4/1) with yellowish brown mottles (10YR 5/4–10YR 5/8) and in the other profiles 3 m to 7 m, yellowish brown (10YR 5/4 or 6/4) or brown (10YR 5/3). In all profiles the oxidized zone formed a well-defined transition—a redox interface—toward the underlying unoxidized, grey (5Y 4/1 or 5/1) zone.

#### Nitrate ( $\text{NO}_3^-$ ) and Exchangeable Ammonium ( $\text{NH}_4^+$ )

At the study sites,  $\text{NO}_3^-$  was present in variable quantities (1 to 15 mg  $\text{NO}_3\text{-N kg}^{-1}$ ) within the oxidized zone (Figure 3) and decreased to below the detection limit for the unoxidized zone. Typically, the distribution of  $\text{NO}_3^-$  across the redox interface, as shown for the SBX site, showed fairly high concentrations in the upper part of the oxidized zone, but decreased rapidly within a narrow 1 m zone above the redox interface to values below the detection limit for

the unoxidized zone (Figure 5). Tritium data from the SBX site revealed that the water infiltrating the soil surface since 1963 was recovered  $\text{NO}_3^-$ -free to approximately 5 m below the redox interface (Figure 5). At another 7 sites within the catchment area pore-water from 1963 was found  $\text{NO}_3^-$ -free at 0.5 m to 8 m below the redox interface.

The exchangeable- $\text{NH}_4^+$  level was smaller than 2 mg  $\text{NH}_4\text{-N kg}^{-1}$  within the oxidized zone, but increased within the uppermost (1 m) segment of the unoxidized zone to values below 7 mg  $\text{NH}_4\text{-N kg}^{-1}$  (Figure 4). Moreover, as seen at site SBX increasing concentrations of exchangeable  $\text{NH}_4^+$  were found within the layer with decreasing  $\text{NO}_3^-$  concentrations, just above the redox interface (Figure 5).

#### Iron Oxides, Structural $\text{Fe}^{2+}$ and $\text{Fe}^{3+}$ in Clay Minerals and Soluble $\text{Fe}^{2+}$

The amount of  $\text{Fe}^{3+}$ , either in free Fe oxides or in clay minerals, was 86 to 90% of the total Fe for the

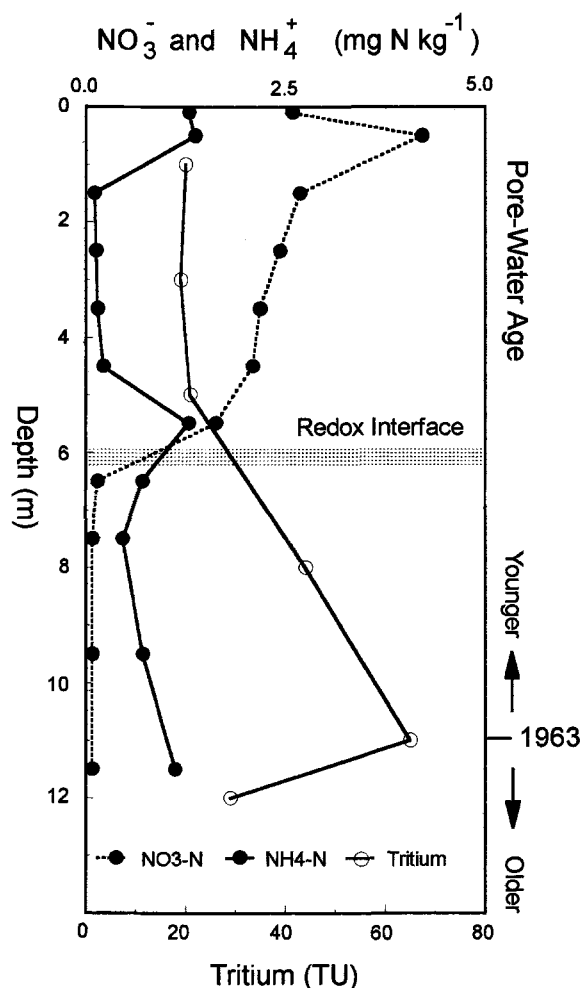


Figure 5.  $\text{NO}_3^-$ , exchangeable  $\text{NH}_4^+$ , and tritium ( $^3\text{H}$ ) isotope vs. depth in profile SBX. Tritium has been abundant in precipitation since 1952 when aboveground nuclear tests began, and reached maximum values in 1963, when nearly all aboveground testing ended. The presence of substantial amounts of tritium in pore-waters therefore identify water which entered the soil surface in 1963.

upper part of the oxidized zone and the amount decreased to about 50% within the unoxidized zone, where  $\text{Fe}^{3+}$  was bound primarily within clay minerals (Figure 6). Free Fe oxides were not detected in this zone. The Fe remaining was structural  $\text{Fe}^{2+}$  within the clay minerals, and the amount increased markedly at the redox interface (Figure 7). The content of structural  $\text{Fe}^{2+}$  for clay minerals (Figure 7) was fairly constant, 10 to 14%, in the upper part of the oxidized zone, but increased evenly within a 2 m wide zone above the redox interface, to about 50% in the grey unoxidized zone. The distribution of exchangeable  $\text{Fe}^{2+}$  was similar to that of structural  $\text{Fe}^{2+}$  in clay minerals, that is, the content of exchangeable  $\text{Fe}^{2+}$  was relatively low,  $<5 \text{ mg Fe kg}^{-1}$  for the upper part of

the oxidized zone, but increased within the lower 2 m of the oxidized zone to approximately  $70 \text{ mg kg}^{-1}$  within the unoxidized zone (Figure 8). The total amount of Fe was typically in the range of 1.1% and 1.9% Fe for both the oxidized and the unoxidized zone, and remained unaffected by the oxidation processes (Figure 7).

#### Clay Minerals in Clay Fractions

In the coarse clay fraction (0.2 to  $2 \mu\text{m}$ ) from the oxidized zone, constituent clay minerals were smectite, mixed-layered smectite-illite, illite, kaolinite and vermiculite (Figure 9). Mixed-layered smectite-illite was identified by increased peak intensity between 9.8 Å and 14 Å on XRD patterns of the air-dried Mg-saturated sample. In the unoxidized zone, the composition was slightly different, as small amounts of chlorite ( $<10\%$ ) were found (13.8 Å, K-300 °C) (Figure 9). The distribution of illite, vermiculite and chlorite changed across the redox interface (Figure 10). Peak areas of illite (28 to 30%) and chlorite (9 to 11%) were larger for the unoxidized zone, whereas only traces of vermiculite were detected. Relative peak area of vermiculite for the oxidized zone was 22%.

The clay minerals present in the fine clay ( $<0.2 \mu\text{m}$ ) at the redox interface were the same as within the coarse clay (Figure 9), but the amounts were different. Smectite was the most common mineral (41 to 46%) and vermiculite decreased slightly to about 15% and chlorite decreased to 6%.

#### DISCUSSION

According to the color of the soil matrix and motles, the subsoil was subdivided into 2 major redox environments, an upper oxidized zone (3 to 7 m) and an unoxidized zone. Thus, the average downward progression of the redox interface during post-glacial time (13 to 14 Ka B.P.) has been 0.02 to 0.05 cm/year, formed primarily by dissolved  $\text{O}_2$  in the recharge water. The geochemical and mineralogical environment in the unoxidized zone probably have remained unchanged during post-glacial time.

The distribution of  $\text{NO}_3^-$  indicated that the oxidized zone may be subdivided into 2 zones: 1) an upper, intensively oxidized zone (oxic-I) with relatively high  $\text{NO}_3^-$  concentrations to about 2 m above the redox interface; and 2) a partly oxidized, suboxic zone (oxic-II) characterized by decreasing concentrations of  $\text{NO}_3^-$ . High, almost constant concentrations of  $\text{NO}_3^-$  in the oxic-I zone showed that  $\text{NO}_3^-$  reduction was limited, probably because of limit quantities of suitable reductants (Ernstsen 1989). In this zone, inherent exchangeable  $\text{NH}_4^+$  was oxidized by the downward progressing oxidation front.

However, the distribution of  $\text{NO}_3^-$  in the underlying, oxic-II zone, about 2 m deep demonstrated that  $\text{NO}_3^-$  reduction processes here controlled the progression of

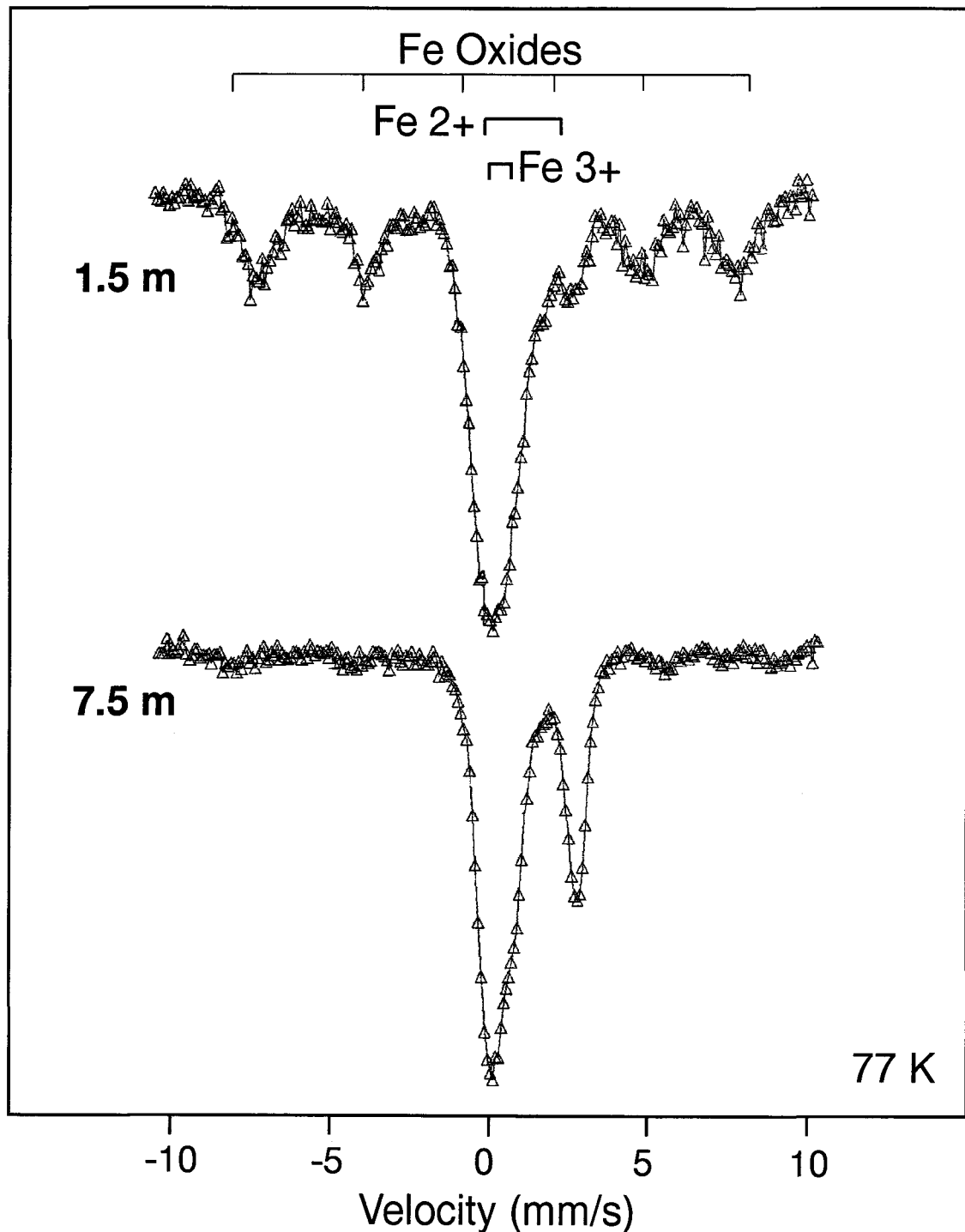


Figure 6. Mössbauer spectra from the oxidized (1.5 m) and (7.5 m) unoxidized zones in profile SBX. Structural  $\text{Fe}^{2+}$  and  $\text{Fe}^{3+}$  in clay minerals and Fe oxides.

$\text{NO}_3^-$ . A 1 to 2 m, oxic-II zone was typical for the SB sites within the catchment area (Ernstsen et al. 1990). Normally the values for exchangeable  $\text{NH}_4^+$  were low within the oxic-II zone, but at 4 of the 11 sites, in-

creased amounts of exchangeable  $\text{NH}_4^+$  were measured.

Occurrence of  $\text{NO}_3^-$  in the oxidized zone and  $\text{NH}_4^+$  in the unoxidized zone was also described by Lind and

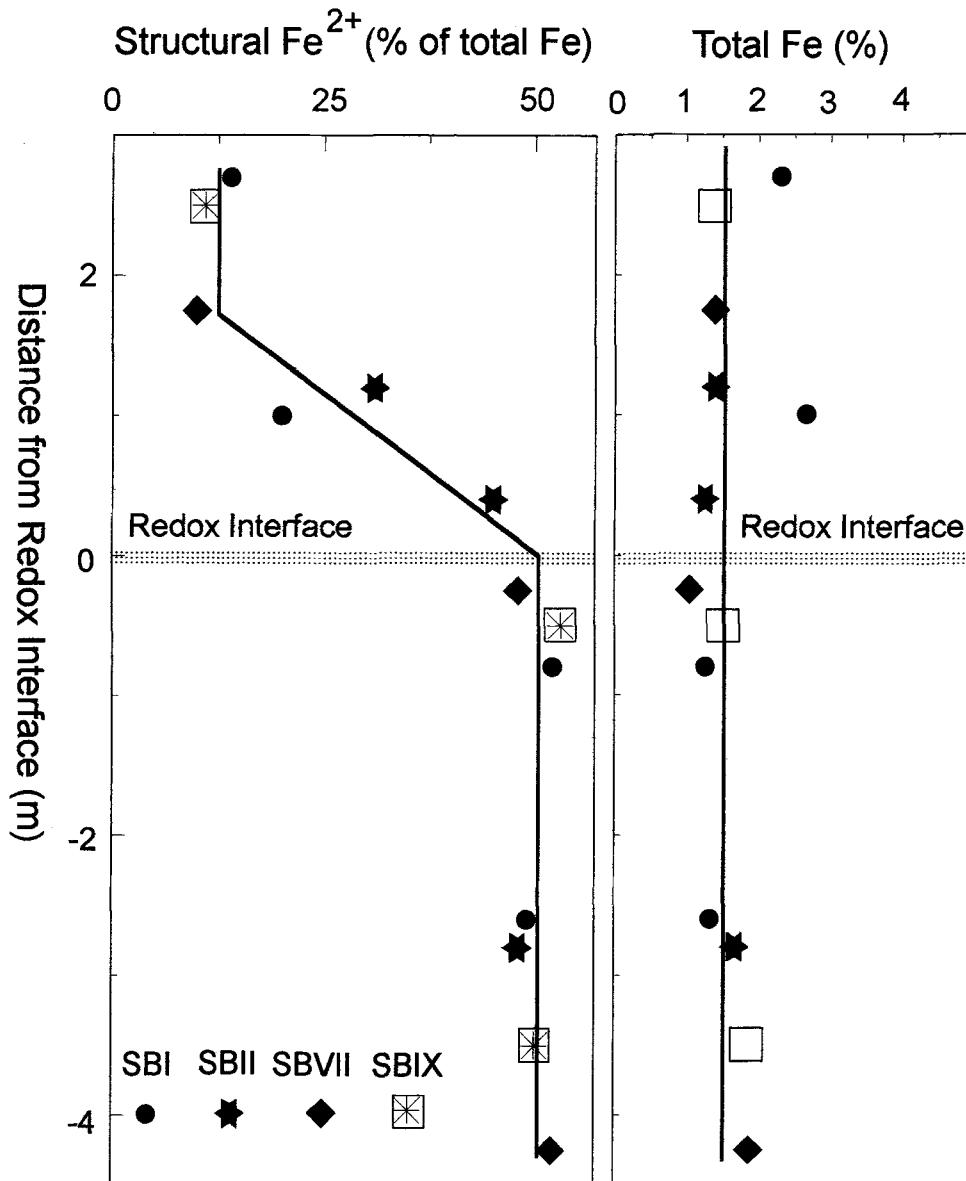


Figure 7. Structural Fe<sup>2+</sup> in clay minerals and Fe-total for the fraction < 2mm vs. depth relative to redox interface.

Pedersen (1976), Hendry et al. (1984), Ernstsen and Lindgreen (1985) and Ernstsen (1989), but in these studies no efforts were made to subdivide the oxidized zone.

Tritium (<sup>3</sup>H) and NO<sub>3</sub><sup>-</sup> profiling at SBX (Figure 5) and another 7 sites revealed that initially NO<sub>3</sub><sup>-</sup>-rich recharge water younger than 1963 was recovered NO<sub>3</sub><sup>-</sup>-free at 0.5 m to 8 m below the redox interface. The uneven downward progression of recharge water was controlled by site specific hydrogeological conditions. Nevertheless, the occurrence of young, NO<sub>3</sub><sup>-</sup>-free water below the redox interface strongly indicates that NO<sub>3</sub><sup>-</sup> reduction occurs.

The distribution of exchangeable and structural Fe<sup>2+</sup> within the oxidized zone supports a subdivision of the oxidized zone into 2 redox environments. In the upper (oxic-I) zone, low amounts of exchangeable Fe<sup>2+</sup> and approximately 10% structural Fe<sup>2+</sup> were present and the remaining structural Fe<sup>2+</sup> is most likely non-accessible or only slowly accessible to the oxidation processes. The amounts of both exchangeable and structural Fe<sup>2+</sup> increase within the brown colored oxic-II zone, thus indicating changes into still more unoxidized redox conditions, for example, lower redox potentials (Patrick and Delaune 1972). As indicated by grey colors, free Fe oxides could not be detected in the

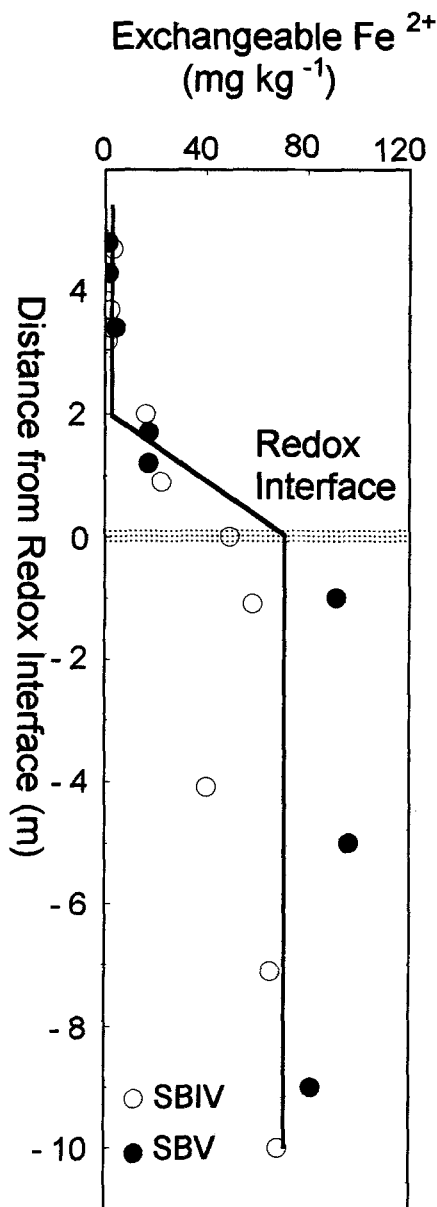


Figure 8. Exchangeable  $\text{Fe}^{2+}$  vs. depth relative to redox interface in profiles SBIV and SBV.

unoxidized zone and Fe existed as exchangeable  $\text{Fe}^{2+}$  or as structural Fe within the clay minerals ( $\text{Fe}^{2+}:\text{Fe}^{3+}$  ratio 1:1). As the geochemical condition within the unoxidized zone probably has remained unchanged during post-glacial time, the initially reduced Fe pool was calculated to be 80 mg exchangeable  $\text{Fe}^{2+}$   $\text{kg}^{-1}$  and 9000 mg structural  $\text{Fe}^{2+}$   $\text{kg}^{-1}$ . After oxidation, the reduced Fe pool in the oxic-I zone declined to approximately 2000 mg  $\text{Fe}^{2+}$   $\text{kg}^{-1}$  and no exchangeable  $\text{Fe}^{2+}$ .

Assuming for the oxidized zone an initial composition of clay minerals similar to the one present today

for the unoxidized zone, the ongoing oxidation processes have changed the composition of the clay minerals, not only for the SBI site (Figure 9). The presence of free  $\text{CaCO}_3$  demonstrates that oxidation processes—and no acidification processes—account for the changes. Chlorite appeared to be a usable indicator mineral for the downward progression of the oxidized zone; that is, chlorite was present within the unoxidized zone only. A close correlation between the progression of the oxidized zone and the presence of chlorite was also noted by Ernstsen and Lindgreen (1985), Ernstsen (1989) and Dixon (1991). A higher content of illite within the unoxidized zone than for the oxidized zone showed that the oxidation processes may also have lessened the amount of illite. Unlike chlorite and illite, vermiculite was present only within the oxidized zone. This, together with the inverse distribution of chlorite plus illite and vermiculite, indicated that vermiculite was formed during the oxidation processes and that chlorite and illite were converted into vermiculite. This process is well-known and described by Melkerud (1984) and Dixon (1990). Changes in the distribution of smectite and in the mixed-layered smectite-illite seems insignificant.

Nitrate reduction may occur in the reduced environment where it is thermodynamically unstable (Korom 1992). However, the process more likely occurred in the oxic-II zone, as evidenced by the decreasing values of  $\text{NO}_3^-$  in a partly oxidized redox environment. In laboratory experiments  $\text{NO}_3^-$  is reduced by soluble  $\text{Fe}^{2+}$  in the presence of either a catalyst (Buresh and Morogham 1976) or at high temperatures (Petersen 1979). Under both of these experimental conditions, the highest activity was obtained at pH 8, corresponding to the pH-value typically measured for the subsoils within the area. This reaction seems limited by the occurrence of rather small amounts of exchangeable  $\text{Fe}^{2+}$  (80 mg  $\text{kg}^{-1}$ ). Much higher amounts of structural  $\text{Fe}^{2+}$  for the constituent clay minerals (9000 mg  $\text{kg}^{-1}$ ) are probably most important for the  $\text{NO}_3^-$  reduction process in the organic-poor sediments. The brown color of the partly unoxidized oxic-II zone shows that free Fe oxides are present. These may transfer electrons within the lattice to the surface of the clay minerals, where the reduction probably transpires (Ernstsen and Lindgreen 1985; Ernstsen 1989). Free Fe oxides, "green rust", are essential for  $\text{NO}_2^-$  reduction (Sørensen and Thorling 1991; Hansen et al. 1994). In addition to the catalytic effect of the free Fe oxides (electron carriers), they may improve the contact between  $\text{NO}_3^-$  ions and negatively charged clay mineral surfaces. Increased values of exchangeable  $\text{NH}_4^+$  within the oxic-II zone is further evidence that  $\text{NO}_3^-$  was reduced in this zone. The reduction capacity evidently was exhausted when about 12% structural  $\text{Fe}^{2+}$  remained, and this remainder may comprise a slowly accessible pool. The major part of the electrons were

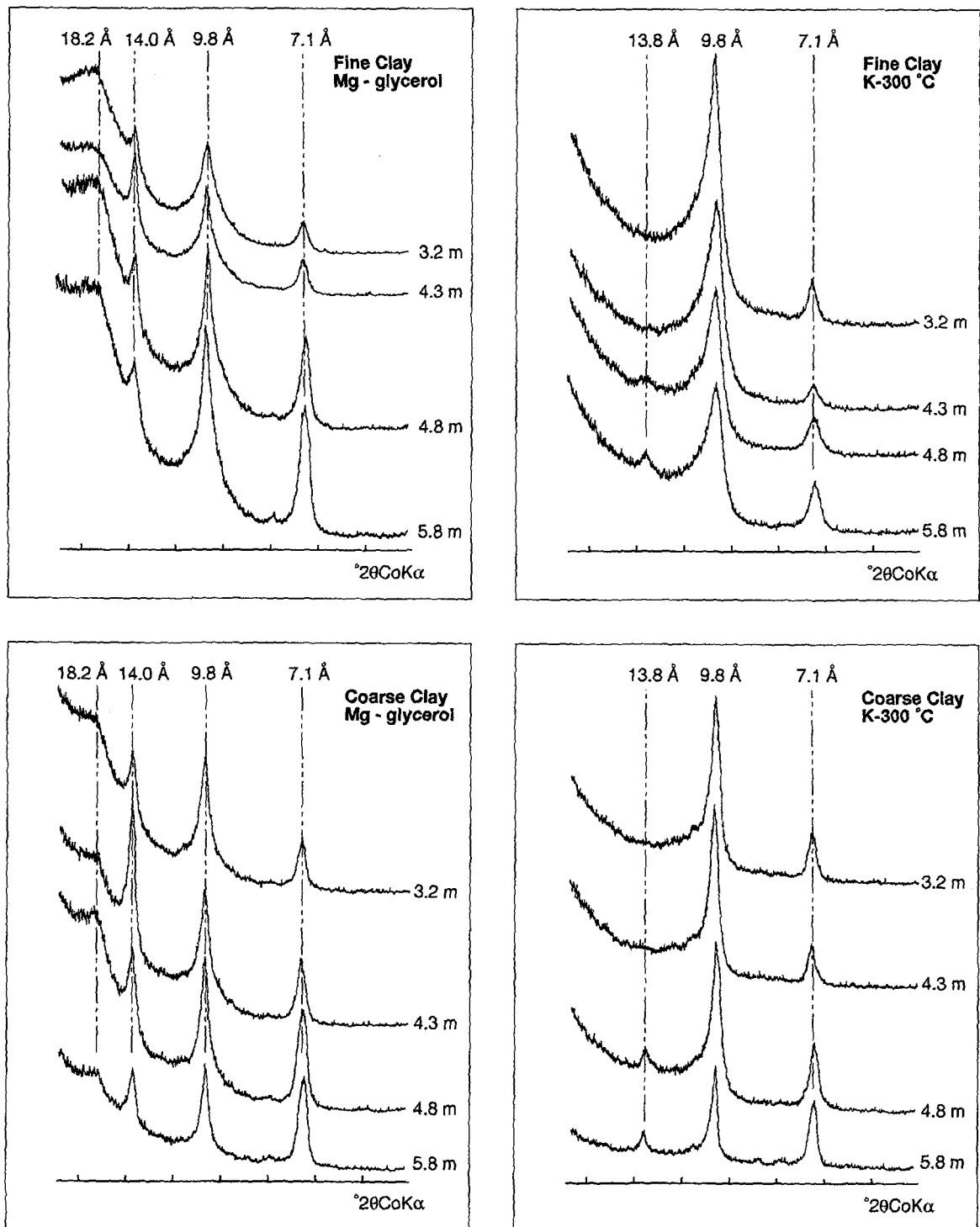


Figure 9. XRD patterns of oriented glycerolated Mg-saturated and heat-treated K-saturated fine clay and coarse clay from profile SBI. Redox interface at a depth of 4.5 m.



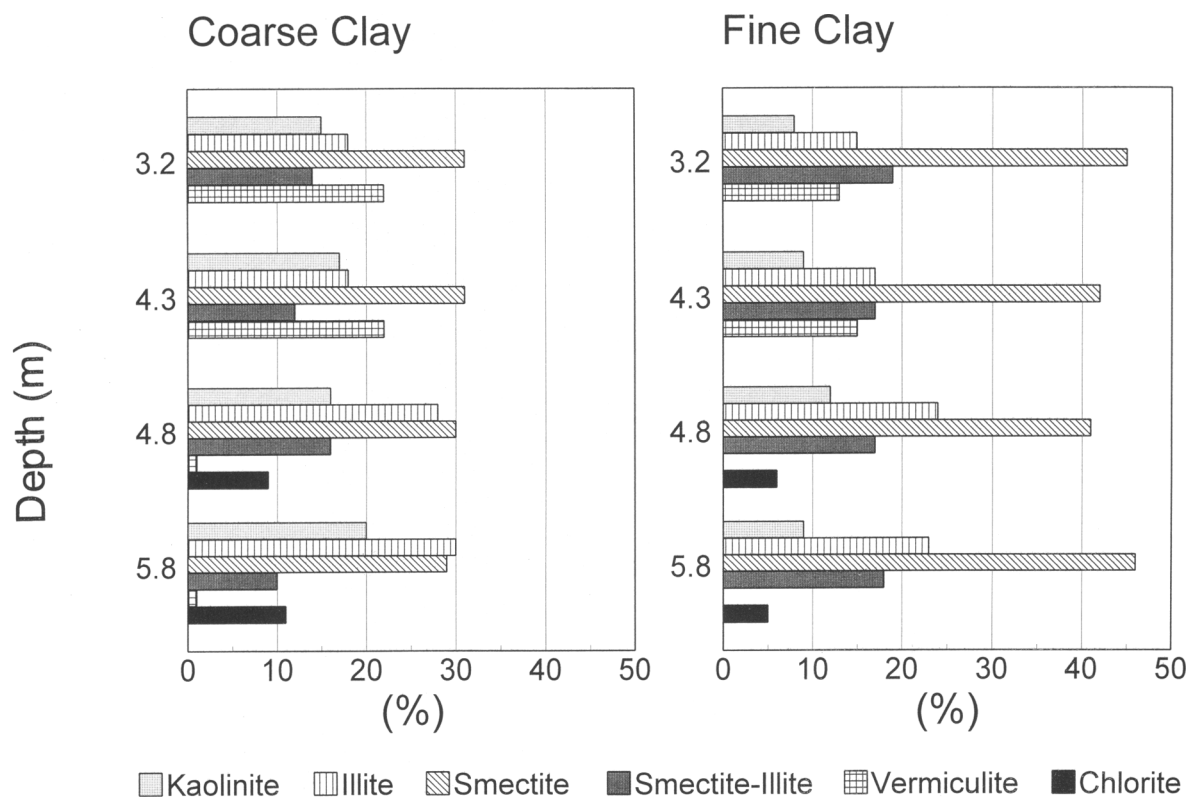


Figure 10. Composition of fine clay and coarse clay from profile SBI shown in Figure 9.

captured during approximately the last 14,000 (post glacial-time), primarily by dissolved  $O_2$  within the leaching water, as the content of other oxidants, for example,  $SO_4^-$  and  $NO_3^-$ , in recharge water below the native vegetation is low (Postma et al. 1991). Because of the dramatic increase in the surface-supplied N, the concentrations of  $NO_3^-$  have increased and the consumption of reductants have increased by a factor of 5 (Postma et al. 1991). This makes the last 50 of  $NO_3^-$  rich water equivalent to 250 of  $NO_3^-$  poor water. Therefore, the geochemical and mineralogical conditions within the oxidized zone were controlled primarily by dissolved  $O_2$  until recently, and the formation of the suboxic, oxic-II zone, evidently has become important for the reduction of  $NO_3^-$ .

### CONCLUSIONS

A close correlation between the distribution of  $NO_3^-$  and reduced Fe within the partly oxidized oxic-II zone above the redox interface of clayey till from Syv Creek strongly indicates that  $NO_3^-$  reduction processes occurs within this zone. Free Fe oxides on the surface of the clay minerals may catalyze the process, there by acting as electron carriers, and increase the contact between  $NO_3^-$  and negatively charged surfaces of the clay minerals. Further investigations are needed to carefully define the oxic-II zone and to describe the

geochemical and mineralogical environment prevailing therein. Also, additional laboratory experiments are needed to describe the process, that is, whether chemical or microbial-chemical.

### ACKNOWLEDGMENT

The author thanks S. Genders, Force Institutes, for his work on tritium, and H. Lindgreen, Geological Survey of Denmark and Greenland, for the Mössbauer spectroscopy analyses. Financial support for the research was provided by the Danish Research Programme on Nitrogen, Phosphorus and Organic matter (NPO 2.2) and the Danish Research Academy (J.nr. 43-4314).

### REFERENCES

- Buresh RJ, Moraghan JT. 1976. Chemical reduction of nitrate by ferrous iron. *J Environ Qual* 5:320-325.
- Christensen W. 1970. Nitrate in surface water and ground water. *Vandteknik* 38:24-29. (in Danish).
- Dixon JB. 1991. Roles of clays in soils. *Appl Clay Sci* 5: 489-503.
- Ernstsen V. 1989. Nitrate reduction in clayey till. Report no. 40. Copenhagen: Geological Survey of Denmark. 69 p. (in Danish).
- Ernstsen V, Gravesen P, Nielsson B, Brüsich W, Fredericia J, Genders S. 1990. Transport and transformation of N and P in the catchment area of Langevad river. Copenhagen: Geological Survey of Denmark. Report no. 44. 63 p. (in Danish).

- Ernstsen V, Lindgreen H. 1985. Inorganic nitrate reduction and reduction capacity of clayey till. Report no.33. Copenhagen: Geological Survey of Denmark. 61 p. (in Danish).
- Ernstsen V, Mørup S. 1992. Nitrate reduction in clayey till by Fe(II) in clay minerals. *Hyperfine Interactions* 70:1001–1004.
- Fujikawa JI, Hendry MJ. 1991. Denitrification in clayey till. *J Hydrol* 127:337–348.
- Hansen HCB, Borggaard OK, Sørensen J. 1994. Evaluation of the free energy for formation of Fe(II)-Fe(III) hydroxide-sulfate (green rust) and its reduction of nitrite. *Geochim Cosmochim Acta* 58:2599–2608.
- Hendry MJ, McCready RGL, Gould WD. 1984. Distribution, source and evolution of nitrate in a glacial till of southern Alberta, Canada. *J Hydrol* 70:177–198.
- Houmark-Nielsen M. 1987. Pleistocene stratigraphy and glacial history of the central parts of Denmark. *Bull Geolog Soc Denmark* 36:3–189.
- Jacobsen OS, editor. 1995. The ground water monitoring programme. Brenderup: Geografforlaget Aps. p 209. (conclusion in English).
- Korom SF. 1992. Natural denitrification in the saturated zone: a review. *Water Resource Res* 28:1657–1668.
- Lind A-M, Pedersen MB. 1976. Nitrate reduction in the subsoil. II. General description of boring profiles, and chemical investigations on the profile cores. *Danish J Plant Soil Sci* 80:82–99.
- Mehra OP, Jackson ML. 1960. Iron oxide removal from soils and clays by dithionite citrate system buffered with sodium bicarbonate. *Clays Clay Miner* 5:317–327.
- Melkerud P-A. 1984. Distribution of clay minerals in soil profiles. A tool in chronostratigraphical investigations of till. *Striae* 20:31–37.
- Munsell Color Company. 1976. Munsell soil color charts. Baltimore.
- Patrick WH, Delaune RD. 1972. Characterization of the oxidized and reduced zone in flooded soil. *Soil Sci Soc Am Proc* 36:573–576.
- Petersen HJS. 1979. Reduction of nitrate by iron(II). *Acta Chem Scan A*:795–796.
- Postma D, Boesen C, Krisiansen H, and Larsen F. 1991. Nitrate reduction in an unconfined sandy aquifer: water chemistry, reduction processes and geochemical modeling. *Water Resource Res* 27:2027–2045.
- Sørensen J, Thorling L. 1991. Stimulation by lepidocrocite (g-FeOOH) of Fe(II) dependent nitrite reduction. *Geochim Cosmochim Acta* 55:1289–1294.
- Zeuthen SB, Vinter FP, Eiland F. 1991. Transport and transformation of and P in the surrounding area of Langvad river. Microbial nitrate reduction in the unsaturated zone. In: Nitrogen and phosphorous in groundwater, B-abstracts. Copenhagen: National Agency of Environmental Protection. p 116–132.

(Received 17 January 1995; accepted 20 December 1995; Ms. 2608)